Journal of Hazardous Materials 189 (2011) 700–709

Contents lists available at ScienceDirect

Journal of Hazardous Materials

journal homepage: www.elsevier.com/locate/jhazmat

Status of aluminium in environmental compartments contaminated by acidic mine water

Wenzhou Lu[a,b], Yingqun Ma[b], Chuxia Lin[c,*]

[a] South China Institute of Environmental Science, Guangzhou 510655, China
[b] Centre for Ecological and Environmental Technologies, South China Agricultural University, Guangzhou 510642, China
[c] Australian Centre for Sustainable Catchments, University of Southern Queensland, Toowoomba, QLD 4350, Australia

ARTICLE INFO

Article history:
Received 2 December 2010
Received in revised form 7 March 2011
Accepted 7 March 2011
Available online 12 March 2011

Keywords:
Aluminium
Acid mine drainage
Stream
Soil
Streambed sediment
Irrigation

ABSTRACT

Investigations were conducted to characterize aluminium in the affected stream and soils downstream of a mine site discharging acidic mine water. The water-borne Al exhibited a highly non-conservative behaviour at water pH below 3.8 in the 0–3.9 km reach and a much more conservative behaviour in the reaches with higher water pHs downstream of the 3.9 km station. The concentration of water-borne Al was higher at the medium flow event than at the flood event in the 0–9 km reach while the opposite was observed for the 16–56 km reach. Transport of Al associated with suspended materials was only observed during the flood event. The amount of Al carried by per unit weight of suspended particles was smaller in the 0–16 km reach than in the 25–56 km reach. The sediment-borne Al increased downstream with maximum Al accumulation occurred in the 25–29 km reach. The residual Al dominated Al fractions in the streambed sediments. The NH_4Cl-extractable Al in the affected soils decreased with increasing distance from the acidic irrigation water source. In contrast, both the water-extractable and total Al in the soils showed no clear distribution pattern. The NH_4Cl-extractable Al was closely correlated with soil acidity while neither total Al nor water-extractable Al was correlated with soil acidity. The vertical distribution of NH_4Cl-extractable Al was regulated by pH with certain influence from soil clay abundance.

1. Introduction

Mine water associated with sulfide minerals is a significant source of sulfuric acid and potentially toxic metals, which may contaminate water, sediments and soils in the areas downstream of the mine sites [1–5]. Acid mine drainage (AMD) has attracted considerable research interest for a few decades and there has been a substantial amount of literature dealing with the chemical behaviours, transport and fates of contaminants in the AMD-affected stream and soil systems [1,6–10]. However, most of the work has been focused on Fe and other heavy metals such as Cu, Pb, Zn, Cd, Mn, As and Ni with relatively less attention being paid to Al.

Aluminium toxicity is an important factor affecting the growth of plant and aquatic biota in acidic ecosystems [11–13]. The available knowledge of Al geochemistry in surface water and soils has been developed largely from acid rain research [14–22]. However, acid rain-affected environments are less acidic, as compared to strongly acidic scenarios frequently encountered in mine environments. Nordstrom and Ball [23] demonstrated a distinct transition of Al^{3+} behaviour from conservative for pH below 4.6 to non-conservative for pH above 4.9 based on speciation calculation of Al in 60 water samples collected from an AMD-affected drainage basin. There is a lack of understanding of the controls on Al chemistry of the highly acidic mine effluent. Besides, free Al ion only accounts for a very small proportion of the total dissolved Al in mine water [24]. To understand the chemical and transport behaviours of Al in the AMD-affected stream systems, non free Al species need to be taken into account in addition to free Al. Alvarez et al. [25] investigated Al fractions in sulfidic mine spoil. To the best of our knowledge, there has so far been no detailed work done on the Al geochemistry in agricultural soils contaminated by acidic mine water.

We investigated Al status in the stream water, suspended particulates and streambed sediments, as well as the soils in the downstream area of a mine site discharging acidic mine water. The objectives were to (a) obtain insights into the spatial and temporal variation in water-borne Al and the spatial variation in streambed sediment-borne Al; (b) understand the transport behaviour and fate of Al in the AMD-affected stream reach; and (c) understand the spatial variation and chemical behaviour of Al in the soil irrigated with the acidic mine water.

* Corresponding author. Tel.: +61 7 46312429; fax: +61 7 46315581.
E-mail addresses: Chuxia.Lin@usq.edu.au, cxlin@scau.edu.cn (C. Lin).

0304-3894/$ – see front matter © 2011 Elsevier B.V. All rights reserved.
doi:10.1016/j.jhazmat.2011.03.018

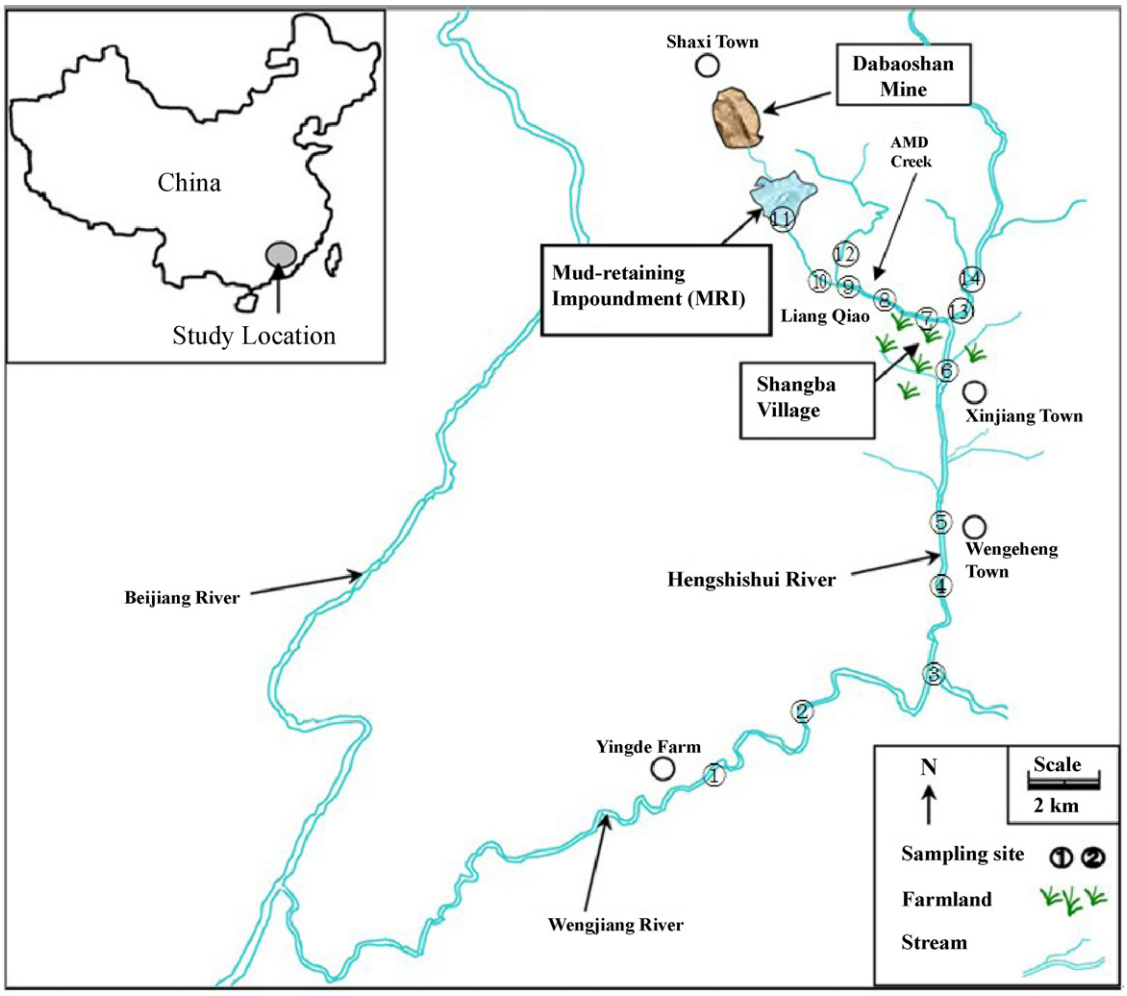

Fig. 1. Map showing the study area and the 14 water sampling locations.

2. Materials and methods

2.1. Study area

The study area (Fig. 1) is located downstream of the mine water discharge point of the Dabaoshan Mine in the northern Guangdong Province, southern China (24°31′37″N; 113°42′49″E). The area experiences a humid subtropical climate. Underground mining of copper ores in the Dabaoshan dates back at least to the Song Dynasty (about 1000 years ago). Since 1970s, large-scale surface mining of iron ore (limonite) has been in operation while smaller scale underground mining of copper, zinc and lead ores (chalcopyrite, sphalerite and galena, respectively) took place simultaneously. As a result of these mining activities, especially the involvement of illegal mining activities in recent decades, large amounts of mine spoils have been left on the land surface and thus are subject to rapid oxidation that leads to acid generation and release of environmentally significant metals. In some mine spoils, the pH was below 0.5 with the concentrations of the soluble Fe, Cu, Zn, Mn and Pb being over 70,000, 1000, 80, 60 and 25 mg kg^{-1}, respectively [26].

To intercept the floodwater and retain the mud being transported from the mine spoil stockpiles on the top of the mountain, a dam wall across the valley was constructed to form a reservoir to trap the sediments (referred to as mud-retaining impoundment i.e. MRI in Fig. 1). The MRI was rapidly filled up with the sediments from the upper catchment due to severe soil erosion and did not have any capacity to hold the mine water during the past decade. Consequently, acidic mine water flows from the dam into a first-order tributary of the Beijing River. This study covers (a) the reaches of the first-, second- and third-order tributaries immediately downstream of the mine water discharge point and (b) the floodplain at the Shangba Village (Figs. 1 and 2) that was irrigated with mine water-affected stream water.

The sampled stream reaches included (a) the unnamed headwater creek draining acidic mine water (referred to as the AMD Creek hereafter) from the southern slope of the Dabaoshan Mine, (b) a 22 km long reach of the Hengshishui River (between the point about 2 km upstream of the junction between the AMD Creek and the Hengshishui River and the confluence of the Hengshishui River with the Wengjiang River), and (c) a 20 km long reach of the Wengjiang River immediately downstream of the junction between the Hengshishui River and the Wengjiang River (refer to Fig. 1). Before the AMD Creek joins the Hengshishui River, there are a few joining small creeks, which were mostly non-AMD-affected. The Hengshishui River originates from a limestone area and the pH of the stream water was frequently above 7 upstream of the junction between the AMD Creek and the Hengshishui River. Downstream of the confluence, the Hengshishui River flows southwards and joins the Wengjiang River at a distance approximately 20 km from the junction between the AMD Creek and the Hengshishui River.

The elevation at the mine water discharge point (Site 11) is 328 m above mean sea level (AMSL). Elevation sharply drops to 163.5 AMSL at Site 10 (about 3.5 km downstream), making the slope of this reach at about 0.06. The reach slope between Site 10 and Site 7, Site 7 and Site 5, and Site 5 and Site 1 was approximately 0.006, 0.003 and 0.001, respectively.

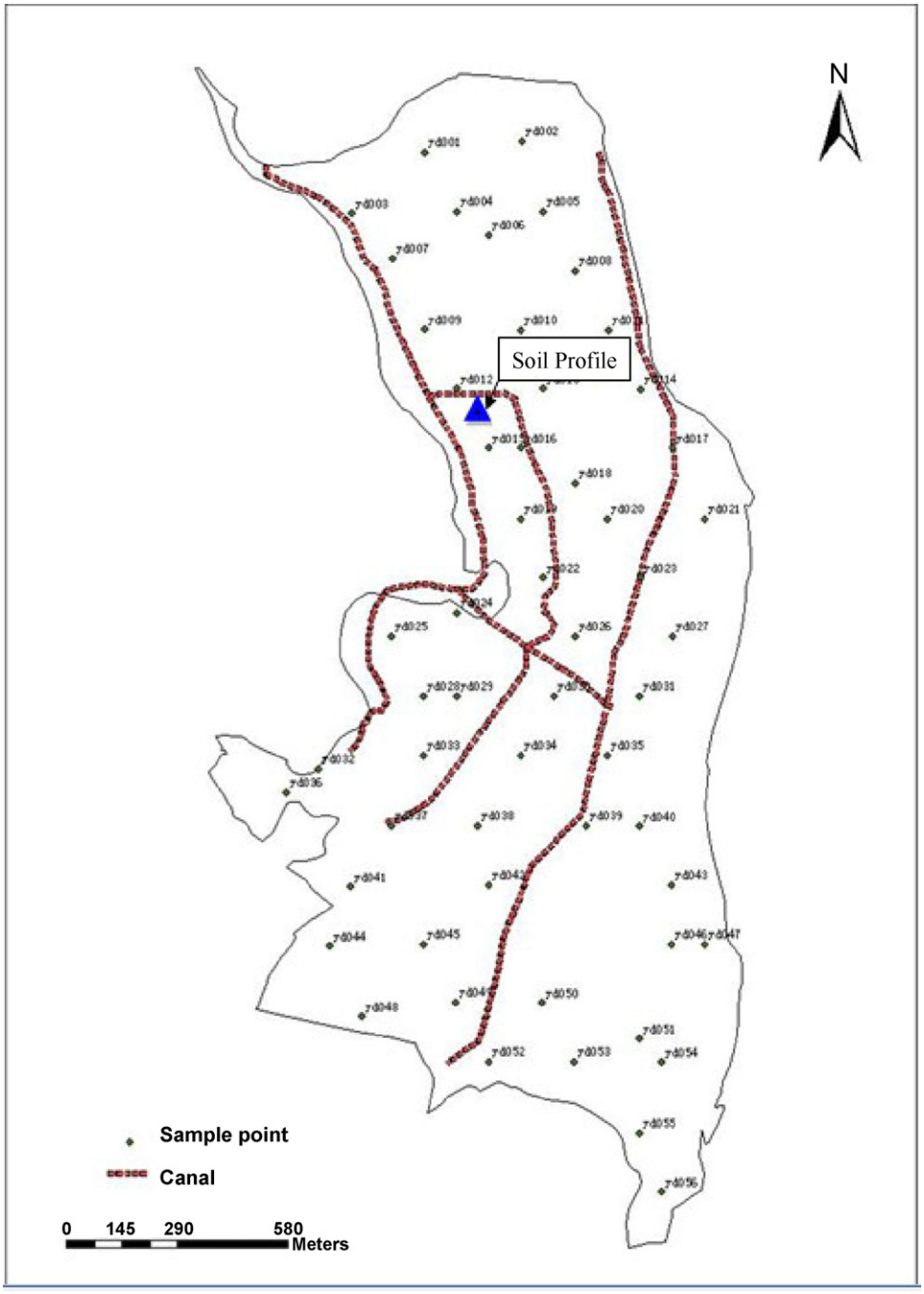

Fig. 2. Map showing the Shangba Village flood plain farmland irrigated with AMD-affected stream water and the locations of the 56 selected soil sample points.

The total area of the investigated floodplain in the Shangba Village is about 153 ha. There is a trend that the surface elevation decreases from northwest to southeast. There were two irrigation water inlet points: one was located near the northwest corner and another was located near the northeast corner of the investigated area. The northwest inlet point received water taken from the AMD Creek at about 6 km from the mine water discharge point while the northeast inlet point received non-acidic water pumped from the Hengshishui River.

2.2. Field methods and sample pre-treatment for stream investigation

Along the investigated transect, 11 sampling locations were established (Fig. 1). Site 11 is located in the MRI, representing the water quality at the mine water discharge point; Sites 10, 9, 8 and 7 are located about 3.5 km, 3.9 km, 6 km and 9 km downstream of the dam wall, respectively; Site 6 is located about 5 km downstream of the junction between the AMD Creek and the Hengshishui River; Sites 5, 4 and 3 are located about 14 km, 18 km and 25 km downstream of the junction between the AMD Creek and the Hengshishui River, respectively; Sites 2 and 1 are located about 10 km and 20 km downstream of the junction between the Hengshishui River and the Wengjiang River. In addition, three reference/control points were established: Site 12 is located about 600 m upstream of the junction between the AMD Creek and the Non-AMD Tributary, representing the water and sediment quality in the Non-AMD Tributary; Sites 13 and 14 are located about 1 km and 2 km upstream of the confluence between the Hengshishui River and the AMD Creek, representing

the water and sediment quality in the main channel of the Hengshishui River before it is affected by the mine water.

Water sample collection for analysis of Al was conducted at various sampling stations during a selected medium flow event (August 13, 2009) and a selected flood event (May 13, 2010). At each site, water sub-samples were collected from at least 3 spots across the river to form a composite sample to represent each sampling location. The composite sample was passed through a filter paper (pore size: 11 μm). The suspended materials retained by the filter paper was air-dried and pulverized prior to analysis. A portion of the filtered water sample was further passed through a 0.45 μm membrane filter. Both filtered water samples (passed through the 11 μm filter paper and 0.45 μm membrane filter) were then acidified to pH <2 with nitric acid, contained in a plastic bottle and stored in a refrigerator prior to chemical analysis. In situ measurements of pH and EC were also conducted during the two sampling campaigns.

Streambed sediment samples were collected from the 14 sampling stations (refer to Fig. 1). At each sampling locations, a composite sample was formed by mixing an approximately equal quantity (on volume basis) of each of the 6 grab samples taken within 50 m^2 to represent each sampling location. The sediment samples were air-dried and ground to pass a 60 mesh sieve.

2.3. Field and mapping methods for soil investigation

Soil sample collection was generally organized into a systematic grid-square sampling pattern (no samples were taken from the places that were occupied by houses). GPS was used to locate the pre-determined sampling spots. The soil sample representing each 80 m × 80 m grid cell was collected at the grid cell centre and was a composite sample consisting of surface soils (0–20 cm) taken from 5 spots within a 2.5-m radius. A total of 295 soil samples was collected from the study area. For the Al study in this article, 56 soil samples were selected for physical and chemical analysis and the selected sample points are shown in Fig. 2.

A combined Kriging and ArcGIS method was used for mapping the distribution of various Al fractions in the study area.

2.4. Test methods for water analysis

In situ pH and EC were measured using a calibrated portable pH meter and EC meter, respectively. The concentration of Al was determined by inductively coupled plasma-atomic optical emission spectroscopy (ICP-OES) using an Agilent 735 Series ICP-OES Spectrometer.

2.5. Laboratory methods for analysis of soils, sediments and suspended materials

For each sample, 1:5 (soil:water) and 1:5 (soil:1 M NH_4Cl) extracts were prepared to determine water-extractable Al (Al_w) and NH_4Cl-extractable Al (Al_{am}). pH and EC in the water extracts were measured by a calibrated pH meter and EC meter, respectively. Total Al (Al_t) was extracted by a multi-acid digestion method; a sample (0.5 g) was initially treated with HCl (10 mL) at 90 °C and subsequently digested with a mixed HNO_3 (5 mL), $HClO_4$ (3 mL) and HF (5 mL) solution at 150 °C on a hot plate for 1 h. The concentration of Al in all the extracts was determined by ICP-OES. Organic carbon content (organic C) was determined using a Walkley–Black method [27]. Water-extractable acidity, NH_4Cl-extractable acidity and total actual acidity (TAA) were determined by the methods of Lin et al. [28,29]. Particle size analysis was conducted using a hydrometer method.

For the sediment samples, the improved BCR sequential extraction procedure [30,31] was used to separate the following three Al fractions: (a) 0.11 M HCH_3COO-extractable metal (termed as Fraction I), (b) 0.5 M $NH_2OH{\cdot}HCl$-extractable metal (termed as Fraction II) and (c) 1 M NH_2CH_3COO-extractable metal after 30% H_2O_2 digestion (termed as Fraction III). The Al concentration in various extracts was determined by ICP-OES. Soluble Al concentration was estimated by the water-extractable Al concentration; exchangeable Al concentration was estimated by the difference between the NH_4Cl-extractable Al concentration and the water-extractable Al; Fraction I is believed to include soluble Al, exchangeable Al and the weak acid-extractable Al. The weak-acid extractable Al was estimated by the difference between Fraction I and the NH_4Cl-extractable Al concentration; Fraction II corresponds to Al bound to oxides of Fe and Mn; and Fraction III consists of organic-complexed Al. The sum of Fractions I–III was used to estimate the total reactive Al fraction. The residual Al fraction after the sequential extraction was estimated by the difference between the total Al concentration and the total reactive Al fraction.

To relate the Al bound to oxides of Fe and Mn (Fraction II), oxide-bound Fe and oxide-bound Mn were determined by ICP-OES using the same extract that was used for determination of the oxide-bound Al.

2.6. Quality control and quality assurance

The Al analyses were conducted by ALS Chemex Guangzhou Laboratory, which has a strict QA/QC procedure in place for all sample analysis, including the use of certified reference material (CRM05-OREAS 45P), duplicates and blanks. For the sediment samples, the analysis of each sample was in triplicate. Repeatability analysis shows that the mean RSD is less than 5% for Al. The mean RSD for organic matter concentration was less than 3%. The detection limit of Al was 1 mg L^{-1}.

2.7. Statistical method

The Pearson's product moment correlational analysis was performed using IBM SPSS Statistics Software Version 13.0.

3. Results and discussion

3.1. Downstream variation of pH and Al in stream water

Spatial variation in stream water pH during the selected medium flow and flood events can be seen from Fig. 3a. Water pH in the 0–9 km reach tended to be lower during the medium flow event than during the flood event while the opposite was observed for the 9–56 km reach. The higher water pH in the 0–9 km reach during flooding is attributable to the dilution of mine-originated H^+ and other acidic cations by substantial amounts of rainwater. However, during non-flood period, the amount of mine water is relatively small and can be rapidly diluted by the water from the upstream Hengshishui River. This explains the higher water pH in the reach below the confluence of the AMD Creek with the Hengshishui River during the medium flow event, as compared to the flood event.

The concentration of water-borne Al was higher at the medium flow event than at the flood event in the 0–3.9 km reach. There was a consistent trend where the Al concentration sharply decreased from the mud-retaining impoundment to the 3.9 km station. Downstream of the 3.9 km station, the water-borne Al concentration was below 10 mg L^{-1} and in the reach between the 25 km station and the 56 km station where water pH was above 5, the water-borne Al was non-detectable or only present in trace amounts. It is interesting to note that Al readings in the water samples filtered by a 0.45 μm membrane and a 11 μm filter paper were very similar to each other, indicating that Al compounds at particle sizes between

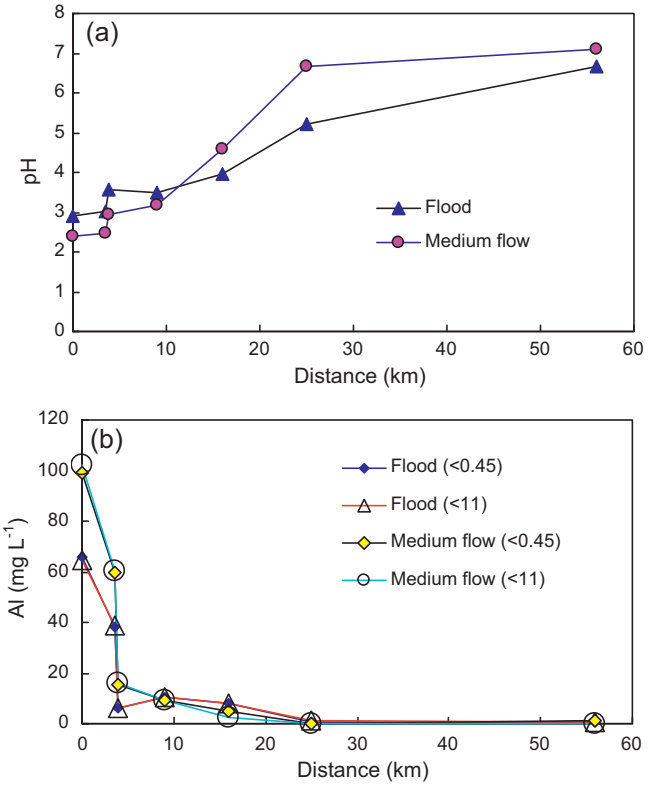

Fig. 3. Spatial variation in (a) pH and (b) Al concentration in the stream water along the investigated transect during a selected medium flood event and a selected flood event; data points from left to right represent Sampling Sites 11, 10, 9, 7, 6, 5 and 1.

0.45 μm and 11 μm were rare in the stream water taken during the two sampling campaigns (Fig. 3b).

The pH dependency of water-borne Al concentration was evident from the above results. The water-borne Al exhibited a highly non-conservative behaviour at water pH below 3.8 (0–3.9 km reach) and a much more conservative behaviour in the 3.9–25 km reach with higher water pHs. This trend is in marked contrast with that predicted by Nordstrom and Ball [23] for Al^{3+}. It is realized that the water-borne Al in this study included forms of Al other than Al^{3+}. As demonstrated by Van Breeman [24] that Al^{3+} species only accounted for a very small proportion of dissolved Al and the aluminium sulfate ions dominated the dissolved Al species in acidic mine water, there is clearly a limitation of using Al^{3+} for geochemical characterization of dissolved Al in acid mine drainage scenarios. The results obtained from this study suggest that rapid precipitation of the mine water-originated dissolved Al could take place at a water pH below 3.8.

The water-borne Al was not detectable at Sites 13 and 14 located in the Hengshishui River reach that is immediately upstream of the confluence with the AMD Creek (Table 1). This indicates that the upstream Hengshishui River (above the confluence with the AMD Creek) was not a source of water-borne Al for the downstream Hengshishui River (below the confluence with the AMD Creek). Consequently, the AMD Creek was the sole source of the water-borne Al occurred in the reach below the confluence of the AMD Creek and the Hengshishui River.

3.2. Spatial variation of suspended material-borne Al

No suspended materials (>11 μm) were obtained for the water samples collected during the medium flow event, indicating that Al transport in the form of suspended particulates is likely to be very limited during non-flooding periods in the investigated stream reaches. During non-flooding periods, the mine water discharging into the receiving stream is mainly derived from the outflowing groundwater, which carries limited amount of suspended materials. The low water level and flow velocity also limit the generation of suspended materials by stream bank erosion. During the sampled flood event in May 2010, varying amounts of suspended materials were obtained from the water samples taken at the sampling locations along the sampling transect. The concentration of suspended materials (in per unit volume of stream water) in the 0–16 km reach was much higher than in the 25–56 km reach. The extremely high concentration of suspended materials at the 9 km station was partly due to severe stream bank erosion, as observed in the field (Fig. 4a). The entry of bank soil materials into the stream markedly increased the sediment load immediately downstream of the eroded sites. It was likely that this also caused the increase in the suspended material-borne Al load (in per unit volume of stream water) as well because the soils in this area are generally rich in aluminium [32]. The majority of the bank-originated suspended materials tended to be deposited rapidly within the 9–16 reach, as indicated by the sharp decrease in the concentration of suspended materials (in per unit volume of stream water) at the 16 km station. In general, the Al concentration in the suspended materials (in per unit weight of suspended materials) was lower in the 0–16 km reach than in the 25–56 km reach. The level of Al in the suspended materials (in per unit weight of suspended materials) remained little change in the 0–16 km reach. There was a sharp increase in the suspended material-bound Al from Site 6 (the 16 km station) to Site 5 (the 25 km station), corresponding to a sudden increase in water pH. The Al concentration in the suspended materials remained stably high all the way downstream to the 56 km station (Fig. 4b). As shown in Section 3.1, the majority of water-borne Al disappeared before the stream water reached the 3.9 km station and the water-borne Al was only present in trace amounts or became non-detectable in the reach downstream of the 25 km station. Therefore, it is unlikely that the increased level of Al in per unit weight of the suspended materials in the reach downstream of the 25 km station was caused by the new formation of Al precipitates from hydrolysis of dissolved Al species. Possibly, differential deposition of suspended particles with different size and density was the major reason responsible for the observed high Al concentration in the

Table 1
Concentration of Al in the water (mg L^{-1}) and streambed sediment (mg kg^{-1}) samples collected from Site 12, Site 13 and Site 14.

Al fraction	Site 12	Site 13	Site 14
Dissolved (water at medium flow event)	UDL	UDL	UDL
Dissolved (water at high flow event)	5 ± 0	UDL	UDL
Water-extractable (streambed sediment)	2 ± 0	16 ± 0	36 ± 3
Exchangeable (streambed sediment)	30 ± 10	UDL	UDL
Weak acid-extractable (streambed sediment)	250 ± 10	90 ± 10	70 ± 6
Oxide-bound (streambed sediment)	580 ± 10	490 ± 20	510 ± 13
Organic-bound (streambed sediment)	599 ± 150	1562 ± 150	1237 ± 230
Residual (streambed sediment)	9400	10,890	12,410

UDL: under detection limit (1 mg L^{-1}).

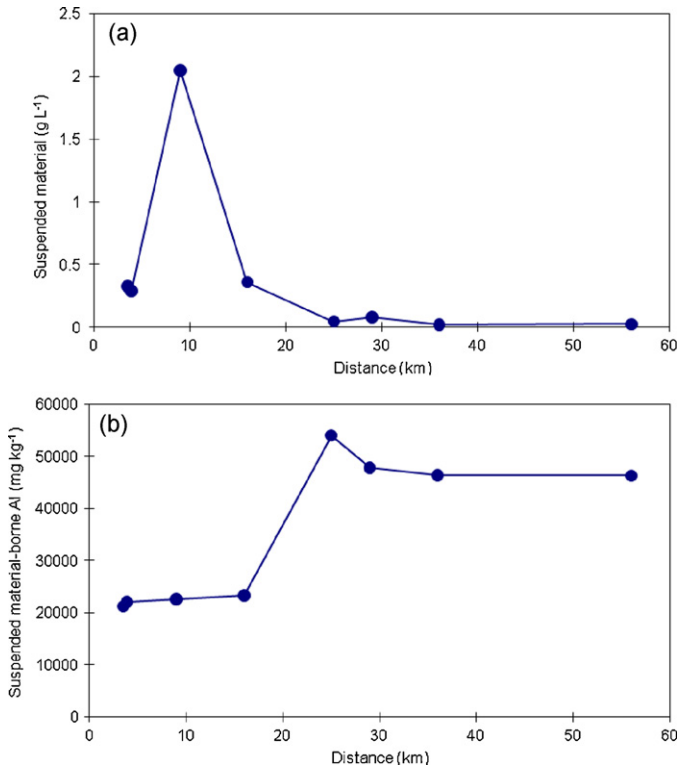

Fig. 4. Spatial variation of (a) concentration of suspended materials in per unit volume of stream water and (b) Al concentration in per unit weight of the suspended materials along the investigated transect during a selected flood event; data points from left to right represent Sampling Sites 10, 9, 7, 6, 5, 4, 3 and 1.

suspended materials in the 25–56 km reach. The suspended materials collected from the 9 km station mainly consisted of quartz and hydrous aluminium silicate minerals (clay minerals) such as muscovite, kaolinite and smectite (our unpublished XRD analytical data). The Al concentration in per unit weight of clay minerals is lower than that of aluminium hydroxides formed due to hydrolysis of soluble Al in the mine water being discharged from the MRI. While the stream bank-originated clay minerals contributed markedly to the total suspended material-borne Al load (in per unit volume of stream water) in the 9–16 km reach, the Al concentration in per unit weight of the suspended materials was low due to the dilution of aluminium hydroxides by non-Al-containing quartz and iron compounds, as well as the lower Al-bearing clay minerals (relative to aluminium hydroxides). The density of quartz, clay minerals and iron compounds is higher than that of aluminium hydroxides. The formers also tend to have a larger size than do the poorly crystallized Al hydroxide colloids formed in the stream conditions. This is supported by the observation that there was a much higher sediment-borne Fe concentration in the 0–16 km reach than in the 25–56 km reach (data not shown). The settlement of heavier and larger-sized suspended particulates in the 9–16 km reach allowed the relative enrichment of lighter and smaller-sized suspended particles, such as aluminium hydroxides in the 25–56 km reach.

During the sampled flood event, no suspended materials were obtained in the water samples collected from Sites 13 and 14 that are located in the upstream Hengshishui River (above the confluence with the AMD Creek), suggesting that the upstream Hengshishui River did not have an input of Al particulates into the downstream Hengshishui River reach (below the confluence with the AMD Creek).

3.3. Fractionation and downstream variation of sediment-borne Al

The sediment-borne Al concentration in the mud-retaining impoundment was very low and this reflects limited precipitation of Al compounds under extremely acidic conditions. There was a trend that the concentration of sediment-borne Al increased downstream with maximum Al accumulation in the sediments occurred in the reach between the 25 km station and the 29 km station. The concentration of sediment-borne Al then decreased downstream (Fig. 5). This downstream variation pattern was in marked contrast with the downstream variation of Al carried by per unit weight of the suspended materials, as shown in Section 3.2. However, in spite of the amount of Al carried by per unit weight of the suspended materials was high in the 36–56 km reach, the content of the suspended materials (per unit volume of stream water) in this reach was extremely low. It is also likely that these suspended Al colloids were of very small-sized and thus tended to settle very slowly and spread over the streambed far downstream. The extensive settlement of the Al-bearing particulates occurred in the 25–29 km reach where the pH (6–7) and flow (low velocity due to smaller slope gradient and bigger channel width) conditions favoured the formation of Al hydroxide-organic matter aggregates, as to be further discussed later in this section. This is also supported by the fact that the streambed sediment-borne Al in the non-AMD-affected upstream Hengshishui River (Sites 13 and 14) was much lower than those at Site 5 (the 25 km station) and Site 4 (the 29 km station) (Table 1),

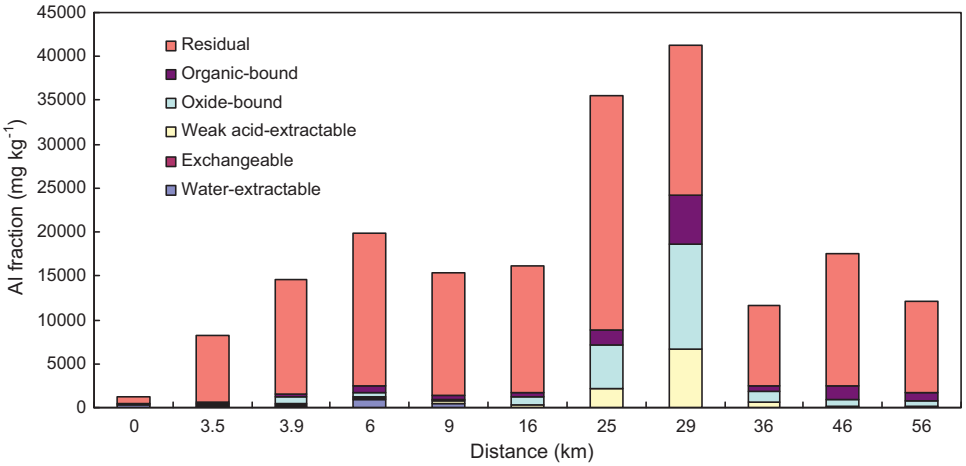

Fig. 5. Fractionation of streambed sediment-borne Al along the investigated transect, from left to right: Site 11, 10, 9, 8, 7, 6, 5, 4, 3, 2 and 1.

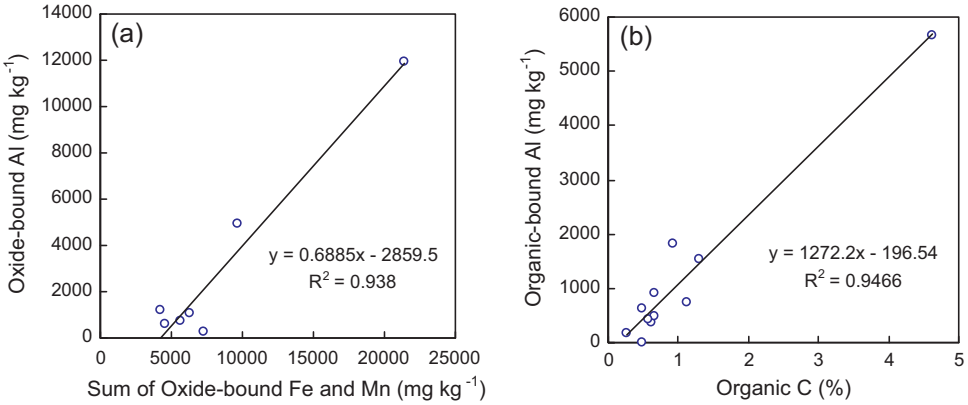

Fig. 6. Relationship between (a) oxide-bound Al and sum of oxide-bound Fe and Mn and (b) organic C and organic-bound Al.

suggesting that the higher concentration of bed sediment-borne Al in the 25–29 km reach was due to the settlement of suspended Al particulates transported from the AMD Creek. As discussed in Section 3.2, substantial amounts of suspended quartz, clay minerals and iron compounds settled in the 9–16 km reach. This was part of the reason for the observed lower sediment-borne Al concentration in this reach, relative to the downstream reach, in addition to the limited settlement of aluminium hydroxides in the 9–16 km reach.

It is worthwhile to note that residual fraction of Al dominated Al fractions in the sediments collected from all locations along the investigated transect. This suggests that much of the sediment-borne Al was present in the structure of primary minerals or well-crystallized Al oxides. Marked presence of the weak acid-extractable Al fraction was limited to the reach between the 25 km station and the 36 km station. Probably, the weak acid-extractable Al consisted mainly of amorphous or poorly crystalline Al hydroxides, which preferably settled in this stream reach due to the favourable pH and flow conditions, as discussed previously. It is likely that the oxide-bound Al was extracted following the collapse of mixed phases of Fe, Mn and Al oxides in the presence of strong reducing agent ($NH_2OH{\cdot}HCl$). There was a good relationship between the oxide-bound Al and the sum of oxide-bound Fe and Mn for the sediment samples collected at the locations downstream of the 9 km station (Fig. 6a), suggesting the possible control of iron and manganese oxides on oxide-bound Al. Although sediment samples upstream of the 6 km station contained considerable amounts of iron oxyhydroxides (data not shown), oxide-bound Al in these samples was negligible possibly due to relatively small particle size and low density, which did not favour the settlement of the colloidal Al. The only exception was at Site 9 (3.9 km) where mixing of acidic mine water with non-acidic water from the Non-AMD Creek might cause co-precipitation of iron, manganese and aluminium hydrous oxides [33] and therefore the presence of oxide-bound Al. Varying amounts of organic-bound Al were observed in the sediments at all locations with maximum accumulation of organic-bound Al occurred at the 29 km station. It is interesting to note that organic-bound Al was closely related to organic C content (Fig. 6b), suggesting the control of organic matter abundance on the formation of organic-bound Al under the investigated stream conditions.

3.4. Soil-borne Al in the irrigation area

The spatial distribution pattern of the water-extractable, the NH_4Cl-extractable and the total Al in the topsoil (0–20 cm) of the investigated floodplain differed markedly from each other (Fig. 7a–c). The NH_4Cl-extractable Al revealed a clear pattern that the concentration decreased with increasing distance from the inlet point of irrigation water (i.e. from north to south). In contrast, both

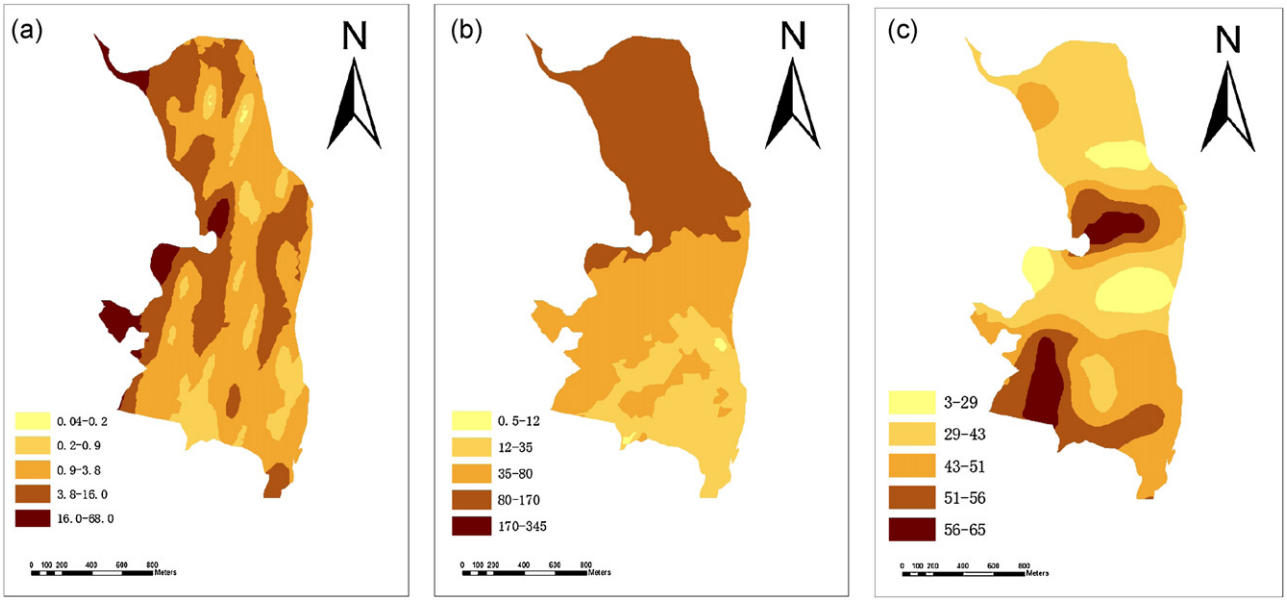

Fig. 7. Distribution map of (a) the water-extractable Al (unit: mg kg^{-1}), (b) the NH_4Cl-extractable Al (unit: mg kg^{-1}), and (c) the total Al (unit: g kg^{-1}),.

Table 2
Correlation coefficients among various Al fractions and other soil parameters ($n = 56$).

	Clay	EC	TA_w	TA_k	TAA	OMC	Al_t	Al_w	Al_{am}
Al_t	0.141	0.133	0.127	−0.002	−0.029	0.006	1.000		
Al_w	0.117	−0.221	−0.029	0.120	0.151	0.083	0.025	1.000	
Al_{am}	0.291	0.104	0.736 **	0.950 **	0.802 **	−0.130	−0.005	0.104	1.000

TA_w: water-extractable titratable acidity; TA_k: KCl-extractable titratable acidity; TAA: total actual acidity; OMC: organic matter content; Al_t: total Al; Al_w: water-extractable Al; Al_{am}: NH_4Cl-extractable Al.
** Significant at the 0.01 level.

the water-extractable Al and total Al showed no clear distribution pattern. Correlation analysis indicated that the NH_4Cl-extractable Al was closely related to various forms of soil acidity while neither total Al nor the water-extractable Al was related to any form of soil acidity (Table 2). These results suggest that the soluble and exchangeable Al were predominantly derived from the mine water and controlled by soil acidity. However, the majority of total Al in the soils was not of mine water origin. The study area is located in subtropical zones where Al is enriched in soils [32]. The mine water-derived Al only accounted for an insignificant proportion of the total Al present in the soils. The poor relationship between pH and the water-extractable Al concentration suggests that the water-extractable Al did not necessarily represent the water soluble Al since in some locations, the concentration of the water-extractable Al was even much higher than the NH_4Cl-extractable Al, which theoretically includes both soluble and exchangeable Al [34]. It was previously observed that the soil Al extracted by deionized water in the study area included Al species of non- or low-charge [35].

Vertical distributions of the water-extractable Al, NH_4Cl-extractable Al, pH, the water-extractable titratable acidity, organic matter concentration and clay content along a selected soil profile are shown in Fig. 8. The water-extractable and NH_4Cl-extractable Al in the top 10 cm of the soil profile were very low but sharply increased downward with the peak occurred at the depth 30–40 cm for the water-extractable Al and at the depth 20–30 cm for the NH_4Cl-extractable Al. Both Al fractions then showed a general

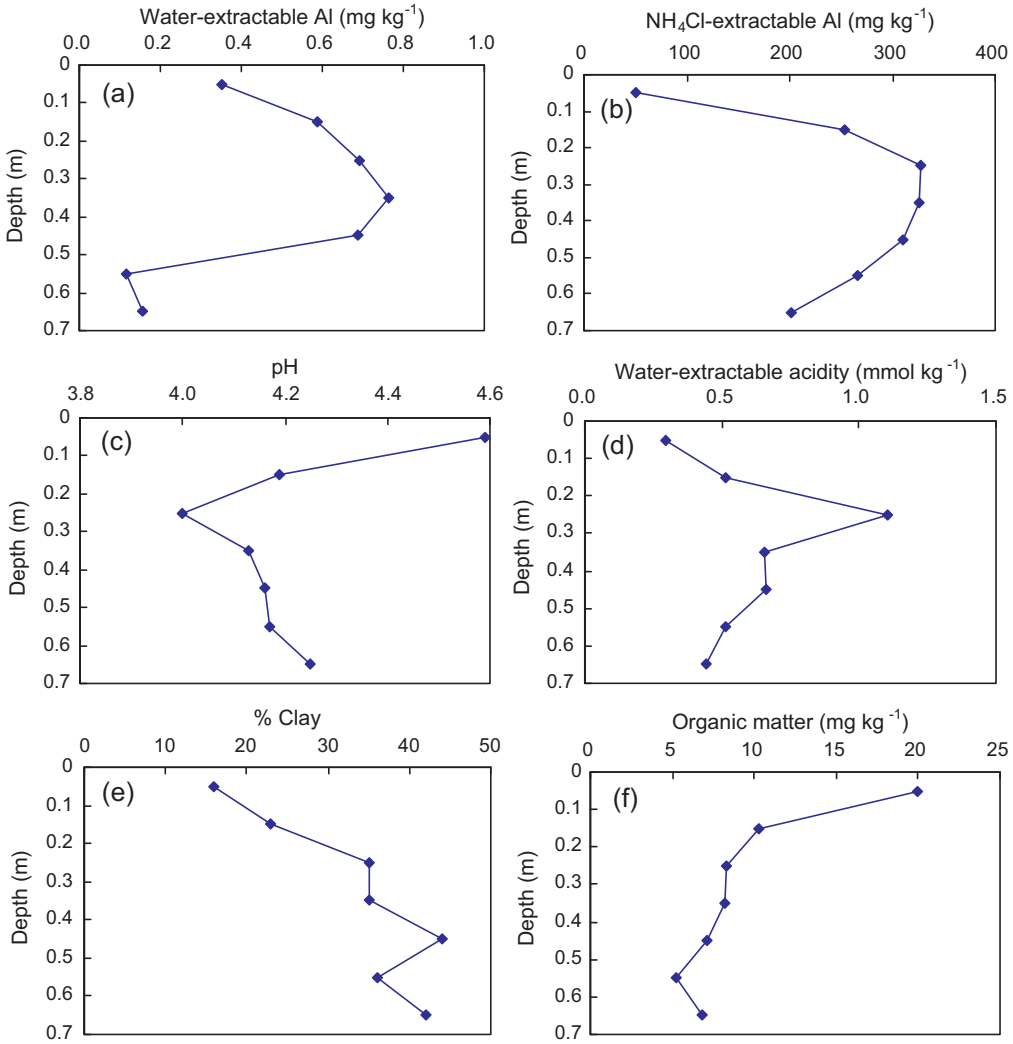

Fig. 8. Vertical variation in (a) the water-extractable Al, (b) the NH_4Cl-extractable Al, (c) pH, (d) titratable water-extractable acidity, (e) clay content, and (f) organic matter concentration along a selected soil profile.

trend to decrease down the profile. The water-extractable Al only accounted for a very small proportion of the NH_4Cl-extractable Al (Figs. 8a and b), indicating that the NH_4Cl-extractable Al mainly consisted of exchangeable Al. There was a good correspondence between the NH_4Cl-extractable Al and the pH or titratable water-extractable acidity along the soil profile; low pH or high acidity corresponded to high concentration of the NH_4Cl-extractable Al and vice verse (Fig. 8c and d). This suggests that the vertical distribution of the NH_4Cl-extractable Al was regulated by soil acidity. Since surface irrigation method was practiced in the study area, the mine water-originated mineral acid and Al tended to enter the soil from the land surface. The occurrence of acidity and NH_4Cl-extractable Al maxima at the subsoil layer rather than surface soil layer reflects the downward movement of mine water-derived H^+ and Al along the soil profile. It is likely that during rainfall events, H^+ and Al in the surface layer percolated with infiltrating water. However, due to decreased permeability with depth as a result of increased clay content (Fig. 8e), their penetration to the lower part of the soil profile was impeded. While the surface soil contained the highest organic matter (Fig. 8f), the exchangeable Al concentration was the lowest in the soil profile. This suggests that the organic colloids had a weak role to play in holding exchangeable Al, possibly because of the low density of negative charge on the colloid surfaces under acidic conditions [36]. It is worthwhile to note that the surface soil had the lowest clay content in the soil profile. XRD analysis showed that the clayey materials contained in the selected soil profile mainly consisted of muscovite, smectite and kaolinite (data not shown). This means that the surface soil might have the lowest content of permanent negatively charged inorganic colloids, which was likely to be responsible for the low cation adsorption capacity in the surface soil. It is expected that gradual downward shifting of the exchangeable Al peak will occur with continuous inputs of acidic mine water into the soil system given that the lower part of the soil profile is still well under-saturated with exchangeable Al considering its huge adsorption capacity potentially derived from its extremely high clay content.

4. Conclusion

The water-borne Al exhibited a highly non-conservative behaviour at water pH below 3.8 and a much more conservative behaviour in the reach with higher water pHs downstream of the 3.9 km station. The concentration of water-borne Al was higher at the medium flow event than at the flood event in the 0–9 km reach while the opposite was observed for the reaches downstream of the 16 km station. Transport of Al with suspended materials only occurred during the flood event and the amount of Al carried by per unit weight of suspended particles was smaller in the 0–16 km reach than in the 25–56 km reach. There was a trend that the concentration of streambed sediment-borne Al increased downstream with maximum Al accumulation in the sediments occurred in the reach between the 25 km station and the 29 km station. The residual Al dominated Al fractions in the streambed sediments. The NH_4Cl-extractable Al in the AMD-affected soils revealed a clear pattern that the concentration decreased with increasing distance from the irrigation water source while both the water-extractable and total Al showed no clear distribution pattern. The NH_4Cl-extractable Al was closely correlated to various forms of soil acidity while neither total Al nor the water-extractable Al was correlated to any form of soil acidity. The vertical distribution of exchangeable Al was regulated by pH with certain influence from the clay abundance but no clear impacts from soil organic matter. It is expected that gradual downward shifting of the exchangeable Al peak will occur with continuous inputs of acidic mine water into the soil system.

Acknowledgements

This work was financially supported by the Natural Science Foundation of China (Project numbers: 40471067 and 40773058), the Guangdong Bureau of Science and Technology (Project No. 2005A30402006) and the South China Institute of Environmental Science (Project No. 2009ZX07528-001).

References

[1] S. Boult, D.N. Collins, K.N. White, C.D. Curtis, Metal transport in a stream polluted by acid mine drainage—the Afon Goch, Anglesey, UK, Environ. Pollut. 84 (1994) 279–284.
[2] M. Olias, J.M. Nieto, A.M. Sarmiento, J.C. Ceron, C.R. Canovas, Seasonal water quality variations in a river affected by acid mine drainage: the Odiel River (South West Spain), Sci. Total Environ. 333 (2004) 267–281.
[3] E. Galan, J.L. Gomez-Ariza, I. Gonzalez, J.C. Fernandez-Caliani, E. Morales, I. Giraldez, Heavy metal partitioning in river sediments severely polluted by acid mine drainage in the Iberian Pyrite Belt, Appl. Geochem. 18 (2003) 409–421.
[4] M.A.H. Bhuiyan, L. Parvez, M.A. Islam, S.B. Dampare, S. Suzuki, Heavy metal pollution of coal mine-affected agricultural soils in the northern part of Bangladesh, J. Hazard. Mater. 173 (2010) 384–392.
[5] E.P. Achterberg, V.M.C. Herzl, C.B. Braungardt, G.E. Millward, Metal behaviour in an estuary polluted by acid mine drainage: the role of particulate matter, Environ. Pollut. 121 (2003) 283–292.
[6] S. Suteerapataranon, M. Bouby, H. Geckeis, T. Fanghanel, K. Grudpan, Interaction of trace elements in acid mine drainage solution with humic acid, Water Res. 40 (2006) 2044–2054.
[7] B.A. Kimball, E. Callender, E.V. Axtmann, Effects of colloids on metal transport in a river receiving acid mine drainage, upper Arkansas River, Colorado, U.S.A., Appl. Geochem. 10 (1995) 285–306.
[8] M. He, Z. Wang, H. Tang, Spatial and temporal patterns of acidity and heavy metals in predicting the potential for ecological impact on the Le An river polluted by acid mine drainage, Sci. Total Environ. 206 (1997) 67–77.
[9] N. Lopez-Gonzalez, J. Borrego, J.A. Morales, B. Carro, O. Lozano-Soria, Metal fractionation in oxic sediments of an estuary affected by acid mine drainage (south-western Spain), Estuar. Coast. Shelf Sci. 68 (2006) 297–304.
[10] B.M. Chapman, D.R. Jones, R.F. Jung, Processes controlling metal ion attenuation in acid mine drainage streams, Geochim. Cosmochim. Acta 47 (1983) 1957–1973.
[11] C. Poschenrieder, B. Gunse, I. Corrales, J. Barcelo, A glance into aluminum toxicity and resistance in plants, Sci. Total Environ. 400 (2008) 356–368.
[12] A.B.S. Poleo, Aluminium polymerization—a mechanism of acute toxicity of aqueous aluminium to fish, Aquat. Toxicol. 31 (1995) 347–356.
[13] P. Quiroz-Vazquez, D.C. Sigee, K.N. White, Bioavailability and toxicity of aluminium in a model planktonic food chain (Chlamydomonas-Daphnia) at neutral pH, Limnologica 40 (2010) 269–277.
[14] N.M. Johnson, C.T. Driscoll, J.S. Eaton, G.E. Likens, W.H. McDowell, Acid rain, dissolved aluminum and chemical weathering at the Hubbard Brook Experimental Forest, New Hampshire, Geochim. Cosmochim. Acta 45 (1981) 1421–1437.
[15] S.C. Tam, R.J.P. Williams, One problem of acid rain: aluminum, J. Inorg. Biochem. 26 (1986) 35–44.
[16] T. Larssen, R.D. Vogt, H.M. Seip, G. Furuberg, B. Liao, J. Xiao, J. Xiong, Mechanisms for aluminum release in Chinese acid forest soils, Geoderma 91 (1999) 65–86.
[17] C. Bini, F. Bresolin, Soil acidification by acid rain in forest ecosystems: a case study in northern Italy, Sci. Total Environ. 222 (1998) 1–15.
[18] J.R. Miller, J.B. Andelman, Speciation of aluminum in an acidic mountain stream, Water Res. 21 (1987) 999–1005.
[19] J. Hruska, P. Kram, Aluminium chemistry of the root zone of forest soil affected by acid deposition at the Lysina catchment, Czech Republic, Ecol. Eng. 3 (1994) 5–16.
[20] E. Tipping, C. Woof, P.B. Walters, M. Ohnstad, Conditions required for the precipitation of aluminium in acidic natural waters, Water Res. 22 (1988) 585–592.
[21] J. Mulder, A. Stein, The solubility of aluminum in acidic forest soils: long-term changes due to acid deposition, Geochim. Cosmochim. Acta 58 (1994) 85–94.
[22] G.B. Lawrence, J.W. Sutherland, C.W. Boylen, S.W. Nierzwicki-Bauer, B. Momen, B.P. Baldigo, H.A. Simonin, Acid rain effects on aluminum mobilization clarified by inclusion of strong organic acids, Environ. Sci. Technol. 41 (2007) 93–98.
[23] D.K. Nordstrom, J.W. Ball, The geochemical behavior of aluminum in acidified surface waters, Science 232 (1986) 54–56.
[24] N. Van Breeman, Dissolved aluminum in acid sufate soils and in acid mine waters, Soil Sci. Soc. Am. Proc. 37 (1973) 694–697.
[25] E. Álvarez, M. Fernández-Sanjurjo, X. Otero, F. Macías, Aluminium geochemistry in the bulk and rhizospheric soil of the species colonising an abandoned copper mine in Galicia (NW Spain), J. Soil Sediment 10 (2010) 1236–1245.
[26] W. Lu, C. Lin, Y. Ma, S. Huang, C. Si, Y. Liu, J. Li, Characteristics and potential environmental consequence of weathered materials in the surface layer of a spontaneously combusting mine spoil stockpile, Appl. Geochem. 25 (3) (2010) 496–501.
[27] S.D. Bao, Analytical Methods for Soils and Agricultural Chemicals, China Agricultural Press, Beijing, 2000.
[28] C. Lin, G. Lancaster, L.A. Sullivan, D. McConchie, P. Saenger, Actual acidity in acid sulfate soils: chemical processes and analytical methods, in: C. Lin, M.D.

Melville, L.A. Sullivan (Eds.), Acid Sulfate Soils in Australia and China, Science Press, Beijing, 2002, pp. 65–71.
[29] C. Lin, K. O'Brien, G. Lancaster, L.A. Sullivan, D. McConchie, An improved analytical procedure for determination of actual acidity in acid sulfate soils, Sci. Total Environ. 262 (2000) 57–61.
[30] A. Sahuquillo, S.J.F. Lopez, G. Rauret, A.M. Ure, H. Muntau, Ph. Quevauviller, Sequential extraction procedures for sediment analysis, in: Ph. Quevauviller (Ed.), Methodologies for Soil and Sediment Fractionation Studies, The Royal Society of Chemistry, Cambridge, 2002, pp. 10–27.
[31] P. Matús, J. Kubová, M. Bujdos, V. Stresko, J. Medved, Chemical partitioning of aluminium in rocks, soils, and sediments acidified by mining activity, Anal. Bioanal. Chem. 379 (2004) 96–103.
[32] M.J. Wilson, Z. He, X. Yang, The Red Soils of China: Their Nature, Management and Utilization, Kluwer Academic Publishers, Dordrecht, 2004.
[33] A. Violante, C. Colombo, G. Cinquegrani, P. Adamo, P. Violante, Nature of mixed iron and aluminium gels as affected by Fe/Al molar ratio, pH and citrate, Clay Miner. 33 (1998) 511–519.
[34] C. Lin, G. Maddocks, E. Bateman, M. Clark, D. McConchie, Acidity and major acidic cations in surface soils of a sulfidic mine sites, Australia: implications for mine site rehabilitation, J. Environ. Sci. 10 (3) (2003) 165–173.
[35] A. Chen, C. Lin, W. Lu, Y. Ma, Y. Bai, H. Chen, J. Li, Chemical dynamics of acidity and heavy metals in a mine water-polluted soil during decontamination using clean water, J. Hazard. Mater. 175 (2010) 638–645.
[36] J. Chorover, Zero-charge points, in: D. Hillel (Ed.), Encyclopedia of Soils in the Environment, Elsevier, Oxford, 2005, pp. 367–373.